Pharmaceutical Research, Vol. 22, No. 8, August 2005 (© 2005)
DOI: 10.1007/s11095-005-5272-x

Research Paper

A Novel *in Vitro* and Numerical Analysis of Shear-Induced Drug Release from Extended-Release Tablets in the Fed Stomach

Bertil Abrahamsson,[1,3] Anupam Pal,[2] Marie Sjöberg,[1] Maria Carlsson,[1] Emma Laurell,[1] and James G. Brasseur[2]

Received December 22, 2004; accepted March 25, 2005

Purpose. To design an *in vitro* apparatus that could simulate the *in vivo* range of surface shear stresses relevant for the human stomach under fed conditions.
Methods. Computer simulations were combined with *in vitro* experiments to quantify tablet erosion rate *vs.* surface shear stress. From two separate computer models, of tablets in the fed stomach and of tablets *in vitro*, we first estimated the intragastric range of surface stress and Reynolds number (*Re*), and then designed a dissolution apparatus and parameter space to replicate the *in vivo* conditions. The *in vitro* tablet erosion was determined by a new rotating beaker apparatus that provided predictable surface shear on tablets. Tablet mass erosion rates were measured for two different extended-release tablets at a range of *in vivo* relevant surface shear stresses obtained by varying viscosity of test media and rotation rate of the beaker.
Results. Mass erosion rate and surface shear were found to be highly correlated. Erosion rate increased with surface shear more rapidly at "low" stresses (<35 dyne/cm^2) independent of tablet material. At higher surface stress, erosion was strongly material dependent.
Conclusions. Shear force effects on drug release from matrix tablets relevant for fed state are for the first time possible to predict by in vitro dissolution testing.

KEY WORDS: dissolution apparatus; extended release; stomach.

INTRODUCTION

In vitro drug dissolution testing is a key tool for product development and batch quality control. The value of such investigations is greatly enhanced when the tests provide physiologically relevant data, necessitating *in vitro* replication of the mechanical and chemical environment of the human gastrointestinal (GI) tract at a level relevant to the dissolution process under consideration. Whereas the chemical environments of the GI tract (e.g., pH profiles, bile acids, and ions) have been well characterized (1,2), the hydrodynamic and mechanical environments of the GI tract have received little attention. In the present study, we coupled fluid dynamics computer simulations and experimental data obtained by use of a new *in vitro* method to establish tablet surface shear stress levels relevant for the fed stomach in human. We also determined the effect of surface shear stress on drug release from hydrophilic matrix tablets, a commonly used extended-release (ER) formulation principle. The relationship between gastric fluid motion and drug release is of special relevance to hydrophilic matrix tablets. When such formulations are exposed to the gastric environment, a gel layer forms at the surface by hydration of the hydrophilic polymers. Erosion of this gel layer, and consequent drug release, is susceptible to the details of the hydrodynamic environment. Drug release of poorly soluble compounds from such formulations is fully controlled by surface erosion from hydrodynamic stress and dissolution of the polymer (3,4). Furthermore, the erosion rate and drug release from hydrophilic matrix ER tablets in the stomach has for certain formulations shown to be higher in the fed *vs.* fasting conditions, an effect attributed to differences in hydrodynamic shearing forces acting on the tablet surface (5). These types of tablets were therefore used as model formulations in the present study.

Gastric muscle contraction creates fluid motions that generate forces on tablets tangent ("shear stresses") and perpendicular ("normal stresses") to the tablet surface. Whereas the consequences of the normal stresses have been characterized in humans by using different formulations with different sensitivities to normal forces (6,7), it has not been possible to measure the gastric shear stresses experienced by tablets *in vivo*. Some attempts have been made to indirectly

[1] Preformulation & Biopharmaceutics, AstraZeneca, S-431 83, Mölndal, Sweden.
[2] Department of Mechanical Engineering, The Pennsylvania State University, University Park, Pennsylvania 16802, USA.
[3] To whom correspondence should be addressed. (e-mail: Bertil.Abrahamsson@astrazeneca.com)

ABBREVIATIONS: ER, extended-release; GI, gastrointestinal; MRI, magnetic resonance imaging; *Re*, Reynolds number.

model gastric forces by correlating *in vitro* dissolution and *in vivo* bioavailability data, for example, by varying stirring velocity in a USP apparatus I or II to mimic release profiles measured *in vivo* (8,9). However, these results are very difficult to generalize owing to formulation-specific hydrodynamic effects *in vitro* as well *in vivo*, for example, as a result of density and shape. Thus, understanding of shear forces *in vivo* as well as *in vitro* test methods that approximates physiological hydrodynamics is still lacking.

Preliminary to designing an experimental apparatus and our present experimental protocol, we determined the range of surface shear stresses that an ER tablet is likely to experience *in vivo* in the fed stomach. This was done with computer simulations of the fluid motions and fluid forces in the fed stomach as described by Pal *et al.* (10). The "lattice-Boltzmann" numerical algorithm described in (10) was subsequently advanced to allow the calculation of the motions of finite size ER tablets, and the shear stress on a tablet surface as it moved within a "virtual stomach" during the propagation of contraction waves in the distal stomach (antrum) (11). The computer stomach model (geometry, emptying rate, contraction-wave characteristics, etc.) was parameterized using magnetic resonance imaging (MRI) data of the human stomach in the fed state. From a series of simulations, average shear stress on tablet surfaces was in the range 0–200 dynes/cm^2, with local surface values as high as 500 dynes/cm^2 (11). The computer simulations show that the tablet surface is exposed to a wide range of shear stresses as it moves within the stomach. The tablets undergo high stresses while moving within the antrum and especially when encountering the gastric mucosa. The highest surface stresses occurred when tablets were forced retrograde through advancing antral contraction waves; however, these are rare events and the most probable shear stress values were in the range 10–70 dynes/cm^2.

Knowing the expected range of shear stresses experienced by ER tablets *in vivo*, an aim of the present work was to design a new *in vitro* apparatus with the help of computer simulation with which the experimental parameters could be varied to produce the *in vivo* range of surface shear stresses in the human stomach under fed conditions. To quantify the required experimental parameters, each *in vitro* experiment was replicated precisely on the computer using three-dimensional numerical methods. Once done, the flow around the tablet and the tablet surface shear stress was quantified for each experimental configuration from computer simulation, and the rate of mass loss was quantified from the *in vitro* experiment. A second aim was to quantify the relationship between the *in vivo* relevant shear stress levels and the rate of tablet mass loss for hydrophilic matrix tablets, and to compare these data with a standard pharmacopeial dissolution method.

Hydrodynamics: *In Vivo vs. in Vitro*

Peristaltic contraction waves in the antrum stimulate repetitive gastric flow patterns that, in turn, generate stresses on the tablet surface. The integrated effect of these stresses both transport the tablet within the stomach and degrade the tablet surface (3). The magnitude and distribution of surface shear stress, however, depends on the details of the flow patterns around the tablet including, for example, the existence or nonexistence of a "wake" behind the tablet.

The details of the flow pattern around any moving object are related to a fundamental nondimensional parameter in fluid dynamics called the "Reynolds number." The Reynolds number for the flow of a fluid with density ρ and viscosity μ approaching a tablet with characteristic diameter D with velocity U is given by $Re = \rho UD/\mu$. Reynolds number (Re) is a global, rough order-of-magnitude estimate of the ratio of fluid inertia (flow accelerations) to frictional force in the flow around the object, so that at very small Reynolds numbers ($Re \ll 1$) frictional forces greatly overpower fluid acceleration, and there is no wake behind the tablet. With increasing Re the role of inertia increases and the flow pattern changes. In particular, a steady wake (containing fluid inertia) begins to form behind the tablet and increases in length with increasing Reynolds number. When $Re \sim 10^2$ another change in flow pattern takes place: the flow around the tablet starts oscillating back and forth with time. These oscillations become progressively more chaotic with increasing Reynolds number until, and at very high Reynolds numbers, the flow around the tablet becomes turbulent. At $Re \gg 1$, frictional effects are generally confined to narrow "boundary layers" adjacent to surfaces, and the wake trailing the objects in the flow (12).

Because the changes in flow pattern are accompanied by corresponding changes in shear stress distribution over the tablet surface, it is important to match *in vivo* tablet Reynolds numbers when designing *in vitro* tablet dissolution experiments in order to obtain physiologically relevant results. Typical gastric meal in the fed stomach is viscous liquid with viscosity roughly in the range 10–2000 cP and density not too different from the density of water, often mixed with particulates and semisolids. The characteristic flow velocity is established by the propagation speed of the antral contraction waves, 2–3 mm/s (13,14). Thus, Reynolds numbers of the flow around tablets 1 cm in diameter within the stomach are of order 0.01–30, most likely with occasional short periods of more rapid tablet motion and higher Reynolds numbers. In all cases, however, *in vivo* Reynolds numbers are orders of magnitude below those required for the existence of turbulence. Therefore, to be physiologically relevant, *in vitro* test methods should be designed to produce tablet Reynolds number not too far from the physiological range 0.01–30, and never turbulent.

Conventional *in vitro* measurements of tablet dissolution using the USP II apparatus, for example, are made with water (1 cP) at high stirring rates (50–100 rpm), resulting in a Reynolds numbers of the flow in the beaker itself in the thousands, not only orders of magnitude larger than physiological Reynolds numbers but often large enough to create a highly nonphysiological turbulent flow environment (15,16). Furthermore, the USP II apparatus with rotating paddle generates highly nonuniform eddying flow (15,16) so that a freely moving tablet within can experience high variations in surface shear in an uncontrolled manner. Thus, the flow within the apparatus is physiologically unrealistic, and variability in results can result from unpredictable tablet motions that depend on tablet density and shape, and surface interactions. To obtain predictable and physiologically relevant hydrodynamic conditions it is necessary to fix the tablet position in a well-defined laminar flow at physiological Reynolds numbers.

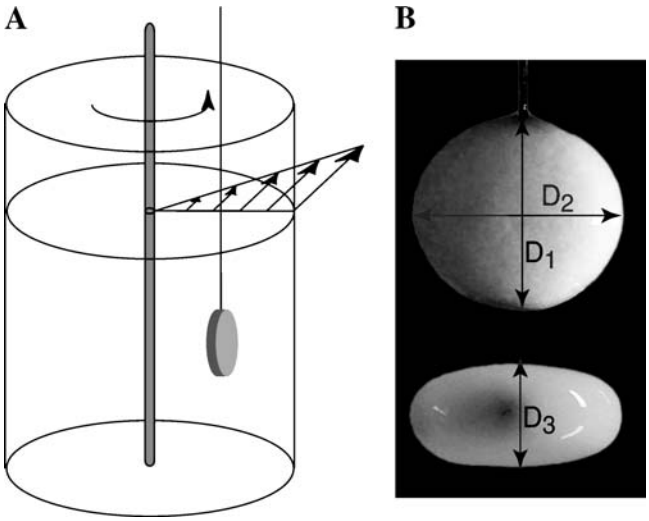

Fig. 1. (A) Illustration of rotating beaker with a tablet fixed on a steel wire. The beaker is glued to the centrally placed rod at the bottom so that when the rod is rotated at fixed rpm the beaker also rotates at the same rpm. (B) Example photographs of a tablet showing the three diameters D_1, D_2, and D_3.

In this work we combined *in vitro* model data with computer model data to correlate mass erosion rate (from *in vitro* experiment) with tablet surface shear stress (from computer simulations of the equivalent flow). The coupled *in vitro*-computer experiment was designed to cover the range of shear stresses experienced by an ER tablet with a roughly similar flow Reynolds number.

MATERIALS AND METHODS

Study Tablets

The present study was performed with hydrophilic matrix extended-release (ER) tablets known to have a sensitive relationship between hydrodynamic conditions and tablet erosion/drug release (3,17). Tablet X was used in most of the experiments. It was ellipsoidal in shape with circular plan form of diameter $D_1 = D_2 = 11$ mm (see Fig. 1A) and aspect ratio $D_1/D_3 = 1.79$, formulated with hydroxypropylmethyl cellulose (HPMC) as the matrix forming agent, containing 10 mg of felodipine. Total initial dry mass was 473 mg. Tablet X was previously studied *in vitro* using standard methods under different conditions, as well as *in vivo* using scintigraphy to estimate tablet erosion (3,18). Another tablet (Y) was also used to investigate the discriminatory power of our new approach of combining *in vitro* with numerical experiments. Tablet Y was also ellipsoidal with planform diameter $D_1 = D_2 = 10$ mm and aspect ratio $D_1/D_3 = 1.69$ and initial total dry mass of 339 mg. Like tablet X, tablet Y was formulated with HPMC, however, with the addition of ethylcellulose and carboxypolymethylene. Tablet Y has also been studied both *in vitro* and *in vivo* with scintigraphic monitoring of tablet erosion (3,5). Results are for tablet X unless otherwise noted.

Design of New Dissolution Apparatus

The rotating beaker design used in the present study is illustrated in Fig. 1A. The design provides a controlled and predictable flow around the tablets with parameters chosen to produce physiologically relevant Reynolds numbers (above). To this end, a beaker 220 mm in diameter was made to rotate at a constant rate between 8 and 50 rpm (Fig. 1A). The beaker was fastened to a stirring rod fixed to the beaker bottom. The ratio of beaker-to-tablet-diameter was 20, ensuring minimal effect of the beaker wall on the flow near the tablet. The beaker was filled with 5000 ml of the test media and a tablet with a drilled hole (0.5 mm diameter) was press-fit onto a stiff steel wire (0.4 mm diameter) fastened rigidly to a steel rod. The tablet was positioned centrally in the test medium 55 mm from the center of the beaker and 40 mm below the free surface. Measurements were made with two tablet orientations: (A) with the flat side of the tablet along the direction of flow and (B) with the flat side perpendicular to the direction of the flow (illustrated in Figs. 3 and 4). The rotating beaker was immersed in a water bath for temperature control. To achieve steady flow the beaker was rotated at least 30 min before an experiment was initiated.

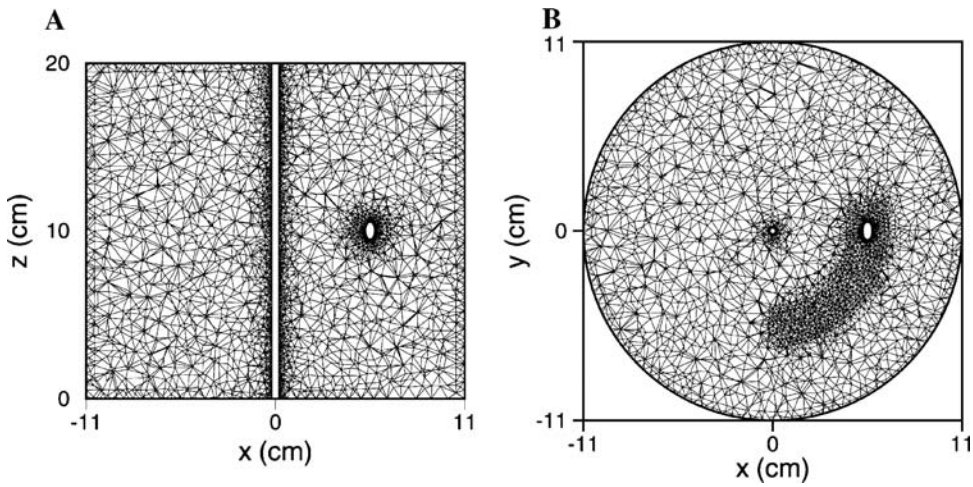

Fig. 2. Cross sections through the computational mesh showing finer mesh near and on the trailing side of a tablet in position A. (A) Vertical cross section. (B) Horizontal cross section.

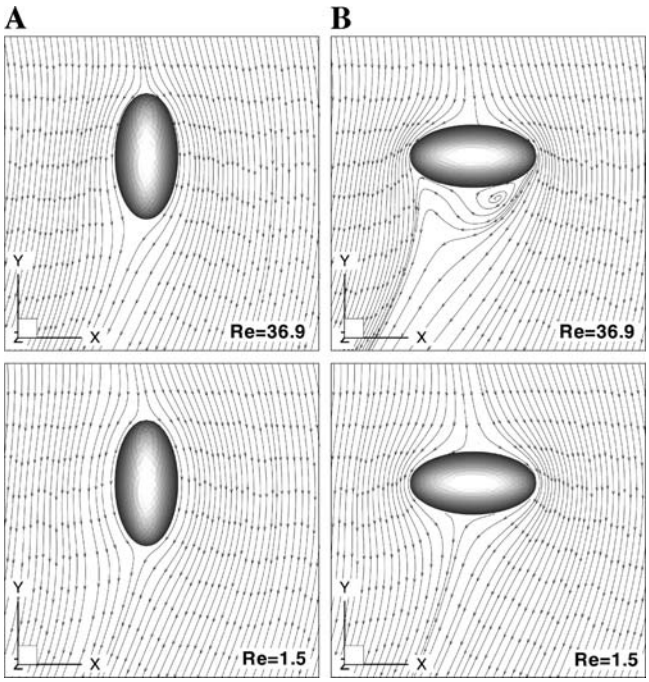

Fig. 3. Simulated streamlines around the tablet in orientations A and B and at Re = 1.5 and Re = 36.9, as indicated. Streamlines are shown on a horizontal plane passing through the center of the tablets.

The choice of the media viscosities and vessel rotation rates were made based on preliminary numerical simulations for tablet orientations A and B that quantified surface shear stress for combinations of vessel rotation rate and fluid viscosity that yielded tablet physiological Reynolds numbers. Knowing the ranges of surface shear stress and tablet Reynolds number encountered by tablets *in vivo* in the fed stomach (see Introduction), experimentally realizable viscosities of test media were coupled with beaker rotation rates limited by the available instrumentation (8–50 rpm) to produce a set of experimental parameters that yielded tablet surface shear stresses over the entire range encountered *in vivo* [10–500 dynes/cm^2 (11)] at flow Reynolds numbers in the physiological range.

Dissolution Media

The dissolution media all contained 0.15 M NaCl (reagent grade, Scharlau Chemie S.A. Barcelona) water solution with 0.5% sodium dodecyl sulfate (SDS) (specially pure, BDH Laboratory Supplies, Pool) and a polymer, end-capped polyethylene glycol (Bermodol PUR 2150®, Akzo Nobel, Stenungsund). Three concentrations (w/w) of the polymer were prepared for the experiments: 1.25%, 2.0%, and 2.75% to obtain three target viscosities: "low" viscosities 25 cP, "medium" viscosities 150 cP, and "high" viscosities 500 cP. Bermodol PUR 2150® was chosen as a viscosity enhancer because solutions created with this polymer have approximately Newtonian behavior (19). SDS was added to suppress phase separation of polymer. Salt concentration levels were chosen to mimic gastric levels.

The viscosities of the test media were measured with a Rheometer (Carri-Med Rheometer CSL^2 100, TA Instruments Ltd., Leatherhead) using an acryl cone (6 cm diameter, 1°). Measurements showed that over 24 h, viscosity typically changed by 4–13% depending on medium viscosity. Because some experiments were performed over multiple days (≤3 days), media viscosities were measured before and after each run; average run viscosities (μ) were used in subsequent analysis. The actual ranges of viscosities used in the experiments were: low 6–50 cP, medium 171–379 cP, and high 486–667 cP. The density of all media (ρ) was 1 ± 0.006 g/cm^3. The mean (range) osmolarity and pH of the media was 339 ± 9 mOsm and 5.4 ± 0.05 pH (micro osmometer 3MO, Advanced Instruments Inc, Massachusetts, USA) which is within the range of possible values in the fed stomach (3). The test media were maintained at 37°C.

Experimental Parameters

The three dissolution viscosities were chosen to produce the *in vivo* range of shear stresses at *in vivo* Reynolds numbers. The numerical simulations showed that, when combined

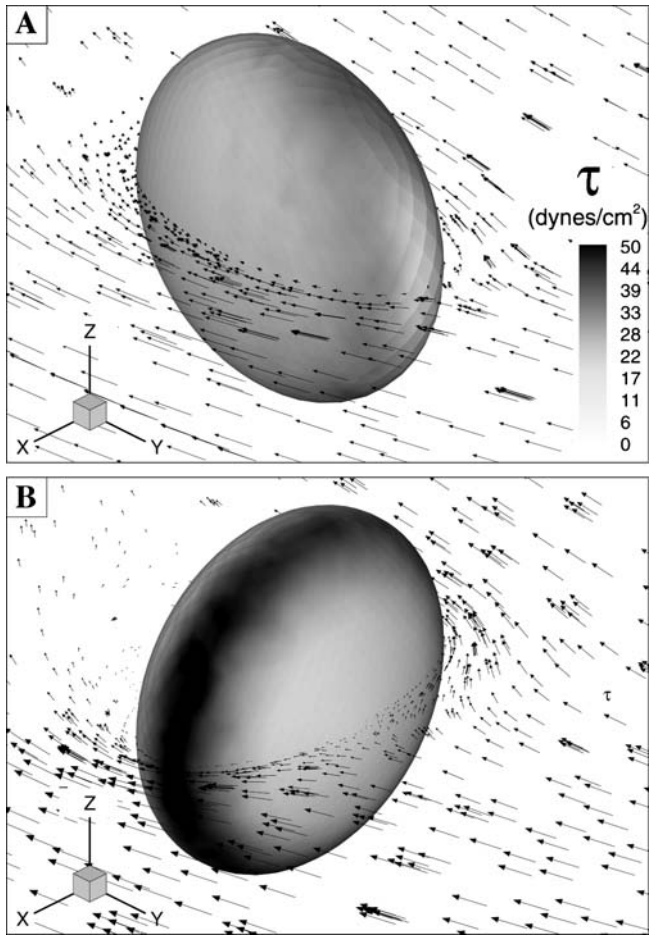

Fig. 4. Grayscale isocontours of local shear stress τ on the tablet surface at Re = 36.9 in orientations A and B (U = 11.5 cm/s, μ = 20 cP). Darker shades of gray indicates higher local surface shear stress and vice versa. The arrows show local fluid velocity vectors in a horizontal plane passing through the center of the tablet. Although the simulations were three-dimensional, velocity vectors are shown in one plane only for clarity. The length and direction of the vectors shows the magnitude and direction of local flow velocity, respectively.

with beaker rotations in the range 8–20 rpm (with low viscosities), 10–40 rpm (with medium viscosities), and 10–50 rpm (with high viscosities), a range of gastric-relevant surface shear stresses were generated *in vitro* at Reynolds numbers within the physiological range. Great effort was made to select experimental parameters at Reynolds numbers that maintain steady laminar flow around the tablet surface near the physiological range. Within the limitations of the instrumentation it was possible to produce tablet Reynolds numbers *in vitro* in the range $Re = (\rho UD/\mu) \sim 0.70–58$, where D is defined as the cube root of tablet volume.

After each experiment the wet tablet was photographed from two sides from which the three major diameters D_1, D_2, and D_3 (Fig. 1B) were measured. Tablet volume was calculated assuming ellipsoidal shape. The characteristic length D of the tablet was defined as the cube root of tablet volume. The rotating beaker design has the advantage that the flow velocity in steady state is precisely known as solid body rotation, that is, linear velocity along circular streamlines, zero at the vessel center and maximum at the wall determined from vessel rotation rate and radius. The relative flow velocity varied between 4 and 30 cm/s. For lower viscosity media beaker rotation speed was limited to 20 to maintain the Reynolds number within the physiological range.

For comparison with the specially designed apparatus, the erosion of tablet X was also quantified in a USP I rotating basket device in 900 ml of 0.15 mM NaCl with 0.5% SDS at 37°C, and 25, 50, and 100 rpm.

Determination of Tablet Erosion Rates

To determine rates of tablet mass loss ("tablet erosion"), tablets were removed from the beaker, dried overnight at 60°C, weighed using an SG balance (Mettler Toledo GmbH Greifensee), then discarded. Tablet mass was measured for 30-, 60-, 90-, 120-, and 250-min periods. Tablet mass loss was calculated for each time period and all experiments were performed in duplicate. Because tablet mass was found to decrease linearly over time (see Results), erosion rates were quantified by linear regression of the erosion-time data. Multiple linear regression (MLR) was used to evaluate the effect of different beaker rotations, medium viscosity and tablet positions using of MODDE® computer software (Umetrics AB, Umeå).

Numerical Experiments Replicating Each Rotating Beaker Experiment

We applied computational fluid dynamics software Fluent 6.0® (Fluent Inc., Lebanon) to simulate each *in vitro* experiment. The geometry of the *in vitro* experiment was replicated precisely and a computational mesh was designed using the grid generation software, Gambit 2.0.4® (Fluent Inc., Lebanon). Figure 2 shows two cross sections through the mesh for tablet orientation A. To resolve the flow near the tablet, a finer mesh was applied near the tablet surfaces (Fig. 2A). A wake is generated on the downstream side of the tablets. To accurately resolve the flow in the wake the finer mesh region was further extended circumferentially on the trailing side of the tablet, as shown in Fig. 2B. The grid contained 172,427 tetrahedral cells and 33,452 nodes. The "no slip" boundary condition (surface velocity = fluid velocity) was applied to the fluid at all surfaces.

To verify that the solution was grid independent, a sample calculation was repeated with twice the number of grid cells. The root-mean-square difference between the two solutions for velocity was <0.025%, verifying the adequacy of the initial grid. To further test the accuracy of the solution, we simulated a spherical tablet in a uniform flow at a low Reynolds number of 1 to compare with published empirical fits (20). The predicted drag was well within the accuracy of the empirical fit (6.1%).

Development of a "Tablet Erosion Model"

This study was directed at quantification of the potential correlations between surface shear stress and tablet erosion rate, and on the development of a "tablet erosion model"—an empirically derived mathematical relationships between tablet mass erosion rate, surface shear stress, relative tablet velocity, medium viscosity, and material properties of the tablet formulation.

We summarize in the Appendix a methodology commonly applied in engineering experimental analysis for estimating empirical equations from multifactorial data using "similarity" requirements between the system being modelled and the experimental system through which data are collected. Here we seek a mathematical representation from which mass erosion rate $\dot{m}$ can be predicted for a given ER tablet of average diameter D that, while moving within in the stomach through gastric fluid of viscosity μ at relative velocity U, experiences average surface shear stress τ_{avg}. This relationship is dependent on the structure (i.e., the physical property of the tablet material, shape, and size) of a particular formulation in resisting surface erosion for given surface shear stress. We parameterize surface material structure with the "ultimate shear stress" τ_u, defined as the critical shear stress above which the gel layer surface fractures. Although we do not explicitly measure this parameter, we include it in the similarity procedure and model its effects implicitly through data collected experimentally for specific formulations.

The procedure described in the Appendix leads to the following two nondimensional empirical equations in symbolic form:

$$\frac{\tau_{avg}}{3\mu U/D} = f(Re), \tag{1}$$

$$\frac{\dot{m}}{\tau_{avg} D^2/U} = g\left(\frac{\tau_{avg}}{\mu U/D}, \frac{\tau_u}{\tau_{avg}}\right). \tag{2}$$

The symbols "f" and "g" imply mathematical relationships that are to be determined from experimental and computer simulation data. For fixed tablet shape and orientation, the nondimensional surface shear stress, $\tau_{avg}/(\mu U/D)$, is mathematically related only to the tablet flow Reynolds number, $Re = \rho UD/\mu$, and we estimate this mathematical relationship from data generated with computer simulation. The symbol "g" in Eq. (2) implies a mathematical relationship between nondimensionalized mass erosion rate $\dot{m}/(\tau_{avg} D^2/U)\dot{m}$, nondimensional surface shear stress $\tau_{avg}/$

($\mu U/D$), and nondimensional "ultimate shear stress" τ_u/τ_{avg}. We estimate the mathematical function g with data from combined *in vitro* experimental measurements of $\dot{m}$ and computer simulation "measurement" of τ_{avg}. All data were collected for tablets in flows with different μ and U, but fixed orientation, size D and material property τ_u.

Once we have determined the mathematical relationship for $\dot{m}/(\tau_{avg}D^2/U)$, we multiply by $\tau_{avg}D^2/U$ to obtain an equation from which mass erosion rate $\dot{m}$ can be predicted from τ_{avg}, D, U, and μ for the specific ER tablet geometry and formulation measured, at the two measured orientations, and over the range of Reynolds numbers covered by the experimental and numerical data used. This final result is the "tablet erosion model." The great advantage is that, whereas the data were collected for specific viscosities, tablet sizes and beaker rotations rates, once the mathematical functions in Eqs. (1) and (2) are found and the accuracy verified (for specific tablet material structure and orientation), the tablet erosion model can be used to "generate" data for *any* variations in tablet diameter, medium viscosity, and relative tablet velocity, so long as the Reynolds numbers and shear stresses are within the range for which the data were collected.

RESULTS

Fluid Flow and Shear Stress on Tablet Surface

Figure 3 shows the streamlines around an ER tablet at orientations A and B in the rotating beaker computed with

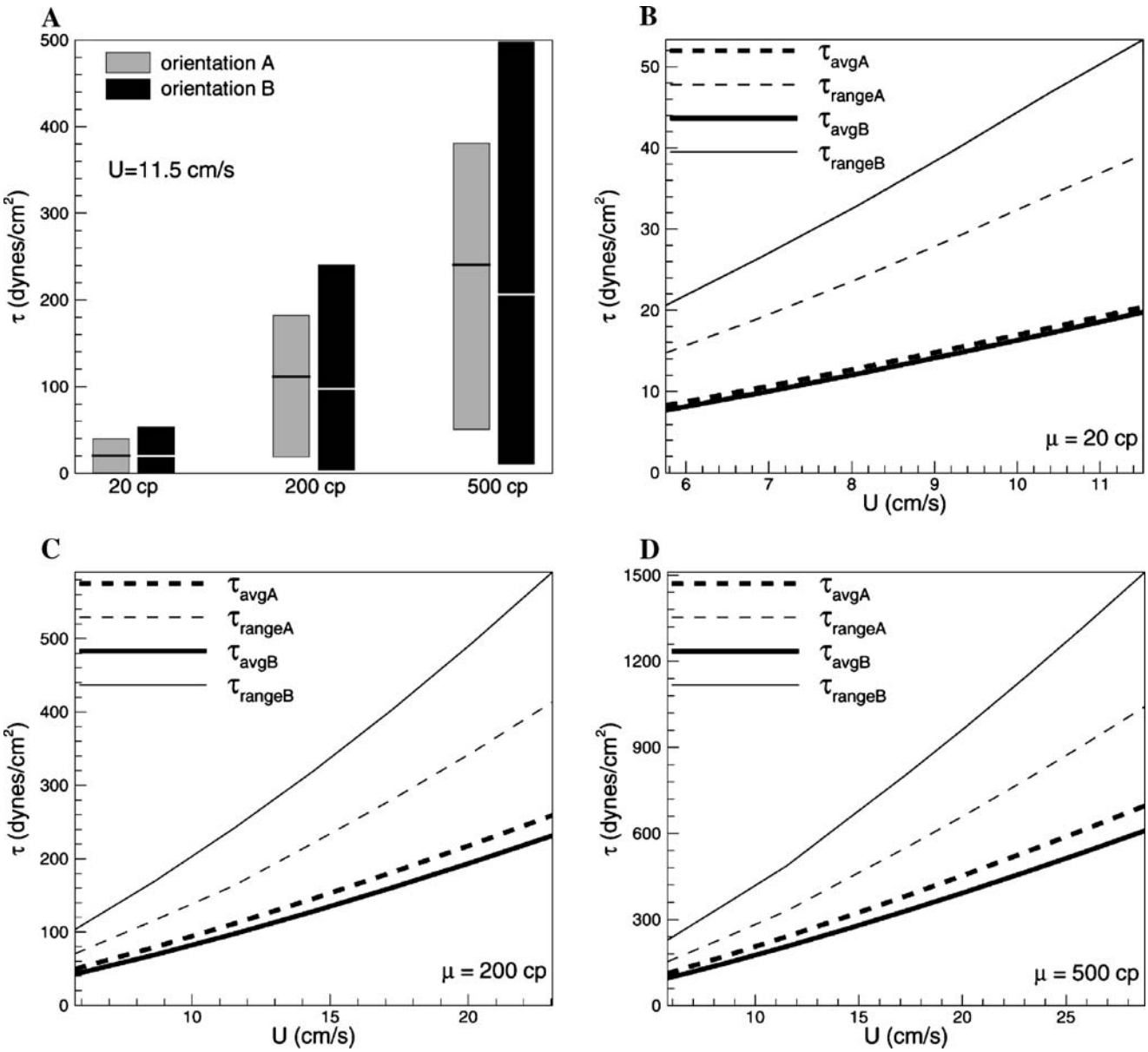

Fig. 5. Local and average shear stress on the tablet surface. (A) Bars show the range of local shear stress and the middle lines give the average surface shear stress. (B)–(D) Variations in local ranges of shear stress ($\tau_{range} = \tau_{max} - \tau_{min}$) and average shear stress (τ_{avg}) with flow velocity at three viscosities of 20 cp, 200 cp, and 500 cp.

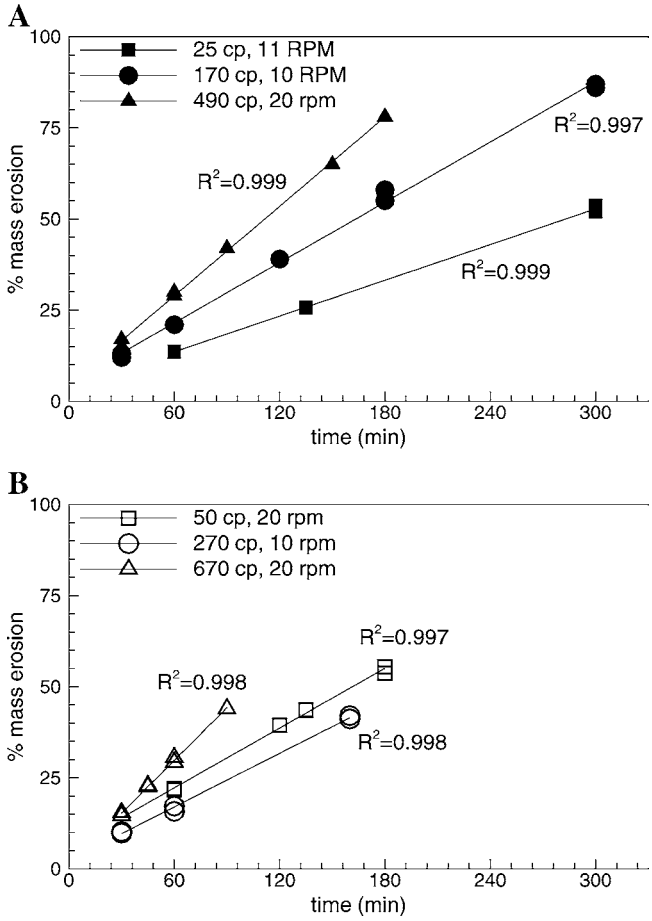

Fig. 6. Examples of experimental measurements that demonstrate the high linear correlation between mass erosion and time for tablets X in orientations A and B, as indicated by figure numbers A and B, respectively. Similar linear erosion-time profiles were obtained in all tablet erosion experiments with $R^2 > 0.97$.

numerical simulation, at Reynolds numbers 36.9 and 1.5. In orientation A the flow pattern around the tablet is similar at the two Reynolds numbers. However, in position B the flow pattern is very different: whereas the streamlines remain attached to the trailing side of the tablet at $Re = 1.5$, at Re 37 the streamlines separate from the sides and form an eddy on the back of the tablet.

Like the flow pattern, the local shear stresses on the tablet surface are also different in different orientations, as shown in Fig. 4 by the isocontours of local shear stress painted on the tablet surface (Re = 36.7). The darker and lighter regions indicate relatively higher and lower surface shear stress, respectively. Similar results are obtained at other Reynolds numbers. Note the high variability in local shear stress over the tablet surface for both orientations A and B. In orientation A, higher shear stresses are produced by the flow on the top and bottom edges of the tablet, and relatively lower values on the trailing edge and sides. By contrast, orientation B has much higher variations in surface shear stress with highest values on the circumferential edges and lowest stresses near the center of the plan form tablet surfaces.

However, whereas the range of shear stresses is greater in orientation A than B, Fig. 5 shows that the average surface stresses are similar. In Fig. 5A the gray and black bars show the range of local shear stress on the tablet surface (τ_{max}, τ_{min}), while the thick central lines show average surface shear stress τ_{avg}, for flow velocity 11.5 cm/s (20 rpm in the *in vitro* experiment) at three viscosities. In each case the range of local surface shear stress is greater with orientation A, but average shear stress in each orientations is comparable. Figures 5B–D show average shear stress τ_{avg} and the range of local shear stress ($\tau_{max} - \tau_{min}$) over the parameter ranges of the *in vitro* experiments. In all three cases the range of local shear stress (τ_{range}) is higher in orientation B than A, but the average shear stress τ_{avg} is similar.

Tablet Erosion

The tablet erosion-time profiles obtained in the beaker were linear as indicated by regression coefficients $R^2 > 0.97$ in all experiments. Examples are shown in Fig. 6 for orientations A and B. This result is consistent with *in vitro* erosion and drug dissolution-time data obtained by other methods for the same formulation (17).

In Fig. 7 percentage change of tablet mass and diameter is plotted against time from all the experiments. Whereas the tablet masses decreased with time, the size of the tablets remained roughly constant because of swelling of the matrix which balanced the mass erosion. Therefore, the volumes (and characteristic lengths) of each tablet were approximated as constant over time in the numerical simulations and calculation of average surface shear stress corresponding to the *in vitro* experiments.

Figure 8 presents isocontours of mass erosion rate $\dot{m}$ and average surface shear τ_{avg} as a function of flow velocity U and media viscosity μ over the parameter space of the *in vitro*–computer experiments with the ER tablets in orientations A and B. Both erosion rate and surface shear stress increased with increasing viscosity and fluid velocity (beaker rotation rate). Multiple linear regression analysis confirmed significant influence of viscosity μ and relative velocity U on

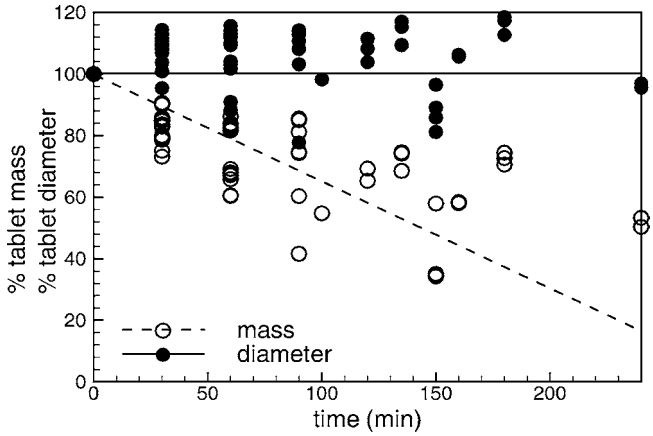

Fig. 7. Changes in tablet mass and diameter D (cube root of tablet volume) with time for each *in vitro* experiment. Although tablet mass reduces with time, tablet diameter remains within ±20%, indicating that absorption of water into the gel layer roughly compensates for volume lost by mass erosion during the period of the experiment.

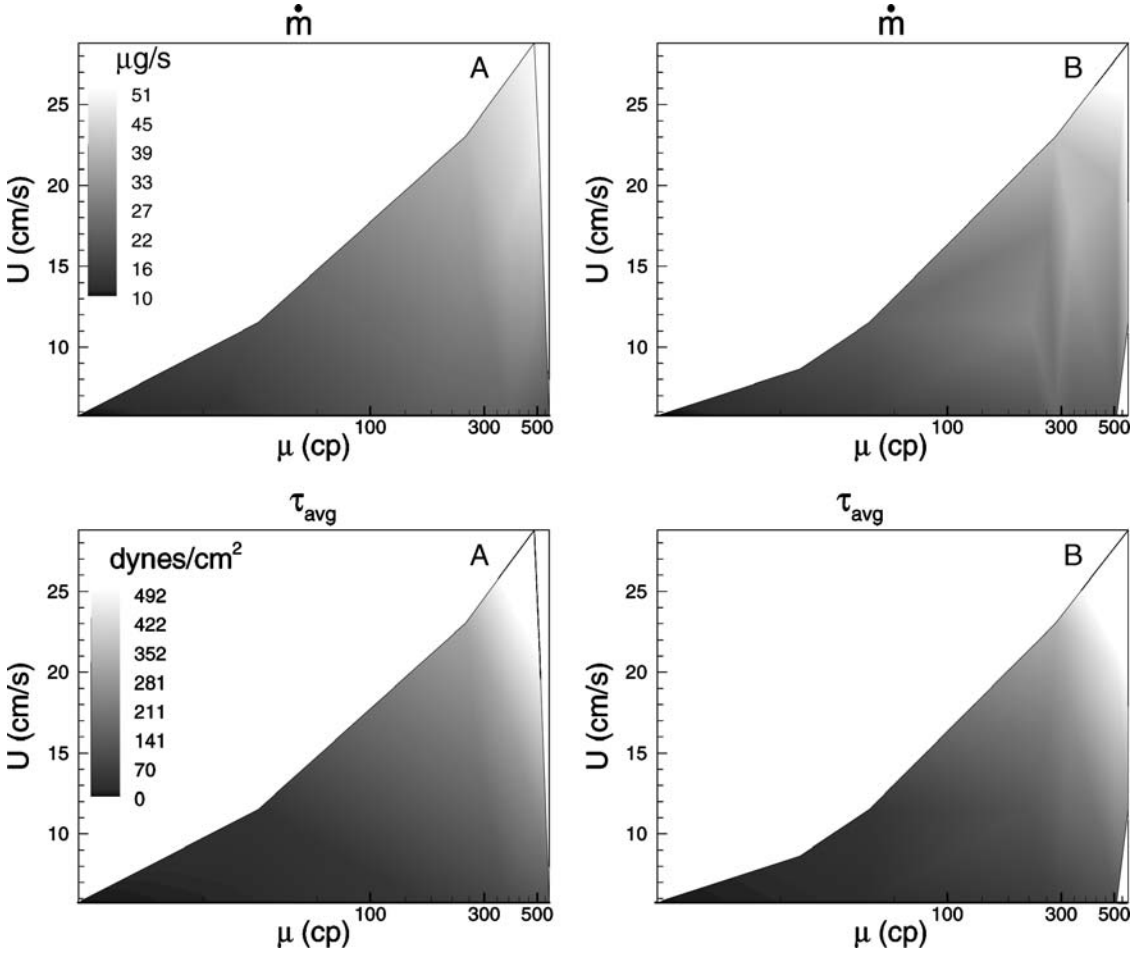

Fig. 8. Grayscale isocontours of rate of mass erosion rate *dm*/*dt* from *in vitro* experiments, and average shear stress τ_{avg} from computer simulation, as a function of relative flow velocity U and fluid viscosity μ, for tablets in positions A and B, as indicated. Erosion rate and shear stress increase with increasing U and μ in a similar manner.

mass erosion rate ($p < 0.001$). However no interaction between these two factors was found, and tablet orientation did not significantly affect the tablet erosion rate ($p > 0.05$), consistent with the numerical experiments where very similar average shear stresses on the tablet surface were obtained for orientations A and B (Fig. 5).

Figure 8 suggests a correlation between tablet erosion rate and average surface shear stress with varying U and μ. This correlation is shown explicitly in Fig. 9 for formulations X and Y, where $\dot{m}$ (normalized by the lowest erosion rate) is plotted against τ_{avg} regardless of fluid viscosity, flow velocity, or tablet orientation. The linear correlations between $\dot{m}$ and τ_{avg} were very high ($R^2 = 0.93$ and 0.89 for tablets X and Y, respectively). Tablet Y degraded a great deal more rapidly than did tablet X for the same levels of surface shear, and the rate of increase in mass erosion rate with surface shear was much more pronounced with tablet Y than X (over the range of shear stress measured, $\dot{m}$ increased by a factor of 10 for tablet Y and a factor of 4 for tablet X). The more robust response of tablet X to surface shear, as compared to tablet Y, is consistent with *in vivo* observations of more rapid tablet degradation and drug uptake with tablet Y when taken concomitant with food, as compared to tablet X (4,11).

Tablet Erosion Model for Tablet X

Following the procedure described in Materials and Methods and outlined in the Appendix, we first determined the mathematical form of the function "f" in equation (1) using data from a series of computer simulations developed to replicate each *in vitro* experiment. From these data we plotted $\tau_{avg}/(\mu U/D)$ against Re and fit the data points with the following parametric form:

$$\frac{\tau_{avg}}{\mu U/D} = B_1 Re^{[B_2 + B_3 \ln(Re)]}. \quad (3)$$

With the least-squares best-fit coefficients B_1, B_2, and B_3 given in Table I for tablet orientations A and B, the accuracy of the fit is nearly perfect ($R^2 > 0.99$). Equation (3) is valid for all ellipsoidal shaped tablets with Reynolds number in the range $Re \sim 0.1$ to 50. The difference in the coefficients B_1, B_2, and B_3 for orientations A and B is only 5–17%, (Table I) confirming the weak influence of tablet orientation on average surface shear stress suggested by Fig. 5.

To determine the empirical function g in Eq. (2) we plotted $\dot{m}/(\tau_{avg} D^2/U)$ against $\tau_{avg}/(\mu U/D)$ and τ_{avg} (using

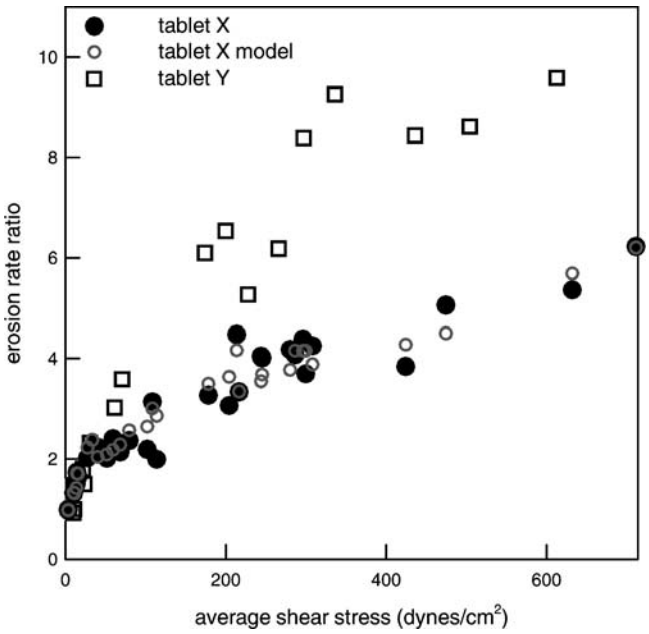

Fig. 9. Correlation of tablet mass erosion rates $\dot{m}$ for tablets X and Y normalized by the lowest erosion rate $\dot{m}$, with average surface shear stress. For tablet X $\dot{m}_0 = 9.5\ \mu g/s$, and for tablet Y $\dot{m}_0 = 10.2\ \mu g/s$.

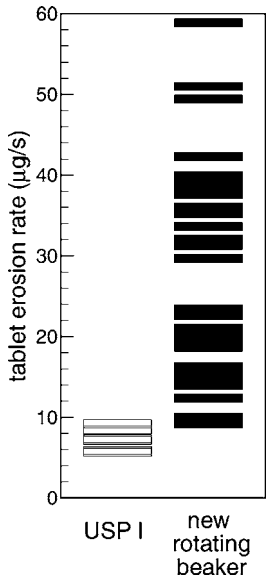

Fig. 10. Ranges of mass erosion rates measured in the USP I apparatus as compared with the current physiologically oriented experimental procedure with a rotating beaker.

isocontours as in Fig. 8) from the data for tablet X, and fit the resulting surface with a polynomial up to second order in $\tau_{avg}/(\mu U/D)$ and τ_{avg}. The resulting expression was then multiplied by $\tau_{avg}D^2/U$ to produce the "tablet erosion model" for tablet X:

$$\dot{m} = \frac{\tau_{avg}D^2}{U}\left[C_1\left(\frac{\tau_{avg}}{\mu U/D}\right)^2 + C_2'\tau_{avg}^2 + C_3'\left(\frac{\tau_{avg}^2}{\mu U/D}\right) + C_4\left(\frac{\tau_{avg}}{\mu U/D}\right) + C_5'\tau_{avg} + C_6\right] \quad (4)$$

The coefficients C_1, C_2',..., generated through least squares fit, are given in Table I ($R^2 = 0.98$). Note that, because τ_u is an unknown constant for all experiments with the same formulation, dimensional τ_{avg} was fit rather than nondimensional τ_{avg}/τ_u, resulting in three of the coefficients, C_2', C_3', and C_5', being dimensional because they incorporate τ_u (see Table I).

Table I. Coefficients of Tablet Erosion Model Relationships. C1–C6 with Eq. (4) are Appropriate Only for Tablet X, while B1–B3 with Eq. (3) are Applicable to Any Ellipsoidal Tablet

Model coefficients	Orientation A	Orientation B
B_1	3.83	3.35
B_2	8.08×10^{-2}	8.52×10^{-2}
B_3	3.12×10^{-2}	3.78×10^{-2}
C_1	3.76×10^{-8}	-2.25×10^{-7}
C_2' (cm^4/dyne^2)[a]	1.10×10^{-11}	1.02×10^{-11}
C_2' (cm^2/dyne)[a]	-4.08×10^{-9}	-7.97×10^{-9}
C_4	3.86×10^{-6}	6.23×10^{-6}
C_5' (cm^2/dyne)[a]	3.58×10^{-9}	1.38×10^{-8}
C_6	-8.22×10^{-6}	-1.09×10^{-5}

[a] As discussed in Results, the fitted coefficients C_2', C_3', and C_5' [Eq. (4)] incorporate the ultimate shear stress, τ_u. The corresponding nondimensional coefficients C_2, C_3, C_5 are related to the dimensional coefficients by $C_2' = C_2/\tau_u^2$, $C_3' = C_3/\tau_u$, $C_5' = C_2/\tau_u$.

The accuracy of the mass erosion model for tablet X is shown by the open circles in Fig. 9, generated with Eq. (4) and the coefficients in Table I at the same conditions as the experimental data points. Whereas linear regression on the data demonstrated strong correlation between $\dot{m}$ and τ_{avg}, Fig. 9 shows that erosion rates increase with surface shear stress much more rapidly at low stress ($\tau_{avg} < 35$ dyne/cm^2) than at higher stresses (τ_{avg} ~35–600 dyne/cm^2). A linear regression line does not capture the low stress behavior, which appears to be relatively independent of formulation type. The mass erosion model, on the other hand, captures both low and high surface shear behavior well. The data and model calculations for tablet X in Fig. 9 were over nearly a factor of 4 in viscosity. Yet the points do not deviate significantly from what is clearly a strong correlation between erosion rate and shear stress. We conclude that there is, at best, a weak influence of viscosity on the correlation between erosion rate and shear stress, captured by the model.

Comparison with USP I

We compared the tablet mass erosion rates for tablet X tested in a standard USP I dissolution apparatus with the current data obtained in a controlled environment calibrated to hydrodynamic conditions relevant to the ER tablets in the fed stomach (Fig. 10). The erosion rates in the USP I apparatus were obtained, as is standard, in water at 25–100 rpm. Whereas the rates of mass erosion measured in the current apparatus were in the range 9.5–59 μg/s, the USP I device measured mass erosion rates of only 5.9–9.5 μg/s, a

narrow range below even the mildest conditions in the current experiments. We conclude that other *in vitro* test designs are necessary to approximate the *in vivo* tablet environment.

DISCUSSION

We have developed a unique experimental procedure that combines numerical simulation with *in vitro* experiment to measure rates of mass erosion of hydrophilic matrix ER tablets in a flow environment designed to approximate the mechanical state of ER tablets in the fed stomach. We have taken advantage, in our experimental design, of both the strengths and the weaknesses of laboratory experiment *vs.* computer simulation. Whereas mass erosion rates are readily measured *in vitro*, measurement of shear stress on the gel layer surface of hydrophilic tablets is not feasible. On the other hand, computer simulation with modern physics-based numerical methods can predict surface stress accurately, but cannot predict surface erosion of arbitrary tablet formulations. We therefore combined the two approaches into a strategy in which tablet erosion is measured in a specially designed *in vitro* apparatus concurrently with "measurement" of tablet surface shear stress with an equivalent computer simulation. We have also used computer simulation to establish an *in vitro* test matrix designed to approximate the surface shear stresses and flow conditions experienced by ER tablets within the fed stomach. With this coupled experimental–numerical strategy we measured tablet erosion rates on two specific ER tablet formulations with fixed geometry and orientation as a function of surface shear stress, relative tablet speed, and medium viscosity at flow conditions relevant to the fed gastric environment. This first-of-its-kind study demonstrates that coupled computer and laboratory experiments are both useful and feasible when fluid and dissolution dynamics interact.

This study has verified that mass erosion, and thereby drug release of a low soluble compound, from hydrophilic matrix ER tablets are highly correlated (R^2 = 0.93 and 0.89) to the average shear stress acting on the tablet gel-layer surface (3). Interestingly, tablet orientation has only a minor influence on the correlations, while the material composition of the formulation can strongly alter the rate at which erosion increases with increasing surface shear stress (Fig. 9). However, when examined in more detail, our measurements on two tablets with very different material properties indicate very different erosion-stress correlation at "low" *vs.* "high" surface shear stresses, below/above roughly 35 dyne/cm^2. At "low" surface shear stresses, the rate of tablet erosion increased much more rapidly with increasing shear stress than at higher surface stresses, however, in a manner independent of tablet structure. At higher stresses (> roughly 35 dyne/cm^2), erosion rates were much higher than at low stresses and erosive behaviour was strongly dependent on tablet structure.

This low-stress/high-stress dichotomy is interesting because computer model simulations of ER tablets in the fed stomach (11) suggest that the most probable average surface stresses, those which wear the tablet surface gradually over long periods of time, are below roughly 40 dyne/cm^2. The current results suggest that this long-time slow degradation of the tablet surface may be independent of tablet structure. The higher stresses are less frequent and degrade the tablet surface much more vigorously for shorter periods of time, but do so in a strongly material-dependent manner.

This dual low–high stress behavior is captured well by the tablet erosion model [Eq. (4)], an accurate empirical equation than predicts the tablet erosion rate of an ellipsoidal tablet with the material structure of tablet X but of arbitrary size D, from specified surface shear stress, relative tablet speed, and medium viscosity. Whereas Eq. (4) is specific to a particular material tablet structure, the mathematical relationship (3) is valid for all ellipsoidal tablets regardless of material composition. With the equation one can predict shear stress on the tablet surface from any specified tablet size and speed, and medium viscosity and density as long as $Re < 60$. On the other hand, the tablet erosion model includes the strong linear correlation between mass erosion rate and surface shear stress given by the data (Fig. 9), it predicts the *nonlinear* interaction between erosion rate and surface stress, and also contains (weaker) dependencies on tablet speed and medium viscosity not included in the linear regression.

The range of shear stresses on ER tablets in the fed stomach is very wide, and consequently tablet erosion rates varied by factors of 4–10 over the physiologically relevant range. This is an important observation that requires attention in the design of specific formulations in order to minimize the impact on drug plasma profiles of concomitant ingestion of food. Interestingly, the present *in vitro* method was able to discriminate between tablets that previously had shown different food sensitivities on tablet erosion that were attributed to hydrodynamic factors (3,5,18). These studies suggest that the differentiation between the tablets not apparent at lower shear stresses, is apparent at higher shear stresses, suggesting that the exposure to high intragastric shear stress in the stomach is sufficiently long to influence overall erosion-time profiles. For this reason, testing by the present method at high shear forces might be useful as a screening tool in early formulation development or as a pilot test to a bioequivalence investigation.

We have shown (Fig. 10) that the rates of erosion measured in the standard way in a USP I device produce significantly lower rates of tablet erosion, and therefore lower levels of shear stress, than does our current experiment, which was designed to approximate *in vivo* levels. We conclude that the more intense shear stresses experienced by a tablet in the fed stomach are not produced with the USP I method. Similar testing in a USP II device was not performed because that apparatus is not suitable for hydrophilic matrix tablets, in part owing to the risk of tablet adhesion to the beaker wall, and in part owing to the nonphysiological flow within the device (16). In contrast, the new experimental approach described here produces both the higher magnitudes of surface shear encountered *in vivo* (Fig. 5), and laminar flows dynamically similar to gastric fluid motions (Fig. 3). Another important advantage of our rotating beaker method over all pharmacopeial methods is the highly controlled hydrodynamic environment it provides, a prerequisite for accurate computer simulation and calculation of surface shear stress.

Although advantageous in its ability to replicate the physiological state, the current rotating beaker method is not

without limitations that warrant scrutiny in future designs. With the current apparatus, for example, only monolithic matrix formulations can be tested. On the other hand, this is the most relevant dosage form for formulations in which drug release is strongly dependent on shear-induced surface erosion. A more practical limitation, however, is that dissolved drug does not distribute uniformly in the bulk of the dissolution medium as the tablet degrades. A nonuniform distribution of felodipine in the beaker was experimentally verified by traversing an UV probe through the beaker during the experiment. Thus, because of the nonuniform concentration of felodipine, the continuous measurement of tablet mass using UV detection of felodipine was not possible. Instead the loss of tablet dry weight was determined after removal of the tablet.

In conclusion, in vitro dissolution testing is now possible under highly controlled hydrodynamic conditions at a flow and with tablet surface shear stresses within the physiological range of the fed stomach. The rate-limiting nature of tablet surface stress for tablet erosion and drug release from hydrophilic matrix ER tablets have been verified and an empirical relationships from which mass erosion rate can be predicted for the formulations tested and surface stress is predicted for any ellipsoidal particle have been developed.

ACKNOWLEDGMENTS

This work was supported by AstraZeneca. We are very grateful to Ms. Lena Wejkum for her contributions to the experiments on tablet Y.

APPENDIX

Development of the "Tablet Erosion Model"

To develop the tablet erosion model we applied a systematic procedure that exists in the engineering literature for developing empirical mathematical relationships between an "independent variable," here the mass erosion rate $\dot{m}$, and the "dependent variables" that affect mass erosion rate (shear stress, relative velocity, fluid viscosity, etc.). This procedure is a combination of "similarity theory" and "dimensional analysis." We can only briefly summarize the method here. The reader should refer to standard textbooks in fluid dynamics (21) for further details.

Two different flows around two different tablets are "similar" if the flow patterns around the tablets are the same. This requires, among other things, that the geometry and orientation of the two tablets in the flow be the same. The tablet size, which we define with D, need not be the same. Neither does the velocity U of the flow relative to the tablet, the fluid viscosity μ, nor the fluid density ρ have to be the same to produce the same flow pattern ("similarity"). Using a process called "dimensional analysis" (21), however, it can be shown that the flow patterns will be the same only if a specific *combination* of μ, ρ, U, and D, given by the "Reynolds number" $Re = (\rho UD/\mu)$, is the same between the two flows.

We applied "similarity theory" with "dimensional analysis" to generalize the development of empirical mathematical relationships from data. We first argued that, for fixed orientation and tablet shape, average surface shear stress τ_{avg} depends only on relative flow velocity U, tablet size D, and fluid properties viscosity μ and density ρ. Dimensional analysis leads to the result that an appropriately nondimensionalized τ_{avg} depends only on Reynolds number. In other words, given sufficient data, we develop a mathematical equation to fit the symbolic form,

$$\frac{\tau_{avg}}{\mu U/D} = f\left(\frac{\rho UD}{\mu}\right) = f(Re). \tag{A1}$$

Dimensional analysis leads to $\mu U/D$ being the appropriate nondimensionalization for τ_{avg}, and the symbol "f" implies a mathematical relationship between $\tau_{avg}/(\mu U/D)$ and $Re = \rho UD/\mu$ that is to be determined from experimental data. In this work we generated this data from computer simulations that replicate the *in vitro* flow. The important point from Eq. (A1) is that to determine an empirical mathematical relationship between τ_{avg}, and the variables U, μ, D, and ρ, we need not vary each of the four dependent variables (U, μ, D, ρ) separately. In this study we vary only μ and U (for fixed D and ρ) to collect data from which we empirically estimate the mathematical relationship (f) between the two nondimensional variables $\tau_{avg}/(\mu U/D)$ and $Re = \rho UD/\mu$. Once done, multiplication of right-hand side of the empirical mathematical expression for f by $\mu U/D$ produces a mathematical relationship between dimensional τ_{avg} and U, μ, D, and ρ.

We applied the same procedure to develop the form of the mathematical relationship between an appropriately nondimensionalized mass erosion rate by arguing that, for fixed tablet shape and orientation, $\dot{m}$ depends only on average surface shear stress τ_{avg}, tablet size D, relative tablet velocity U, a material surface parameter τ_u (see Materials and Methods), and fluid properties μ and ρ. The dimensional analysis procedure leads to the following symbolic relationship:

$$\frac{\dot{m}}{\tau_{avg}D^2/U} = h\left(\frac{\tau_{avg}}{\mu U/D}, Re, \frac{\tau_u}{\tau_{avg}}\right). \tag{A2}$$

Here dimensional analysis lead to the result that mass erosion rate, nondimensionalized by $\tau_{avg}D^2/U$, can be written as a mathematical expression "h" that contains $\frac{\tau_{avg}}{\mu U/D}$, Re and τ_u/τ_{avg}. In this work we determined this mathematical relationship by combining experimental and computer simulation data.

However, we can reduce Eq. (A2) to a simpler form. Assuming that (A1) is uniquely invertible, we replace Re in (A2) with a function that depends only on $\frac{\tau_{avg}}{\mu U/D}$, producing the following reduced form:

$$\frac{\dot{m}}{\tau_{avg}D^2/U} = g\left(\frac{\tau_{avg}}{\mu U/D}, \frac{\tau_u}{\tau_{avg}}\right). \tag{A3}$$

Here "g" implies a mathematical relationship between $\dot{m}/(\tau_{avg}D^2/U)$, $\tau_{avg}/(\mu U/D)$, and τ_u/τ_{avg} that we determine through data obtained by combining *in vitro* experimental measurements of $\dot{m}$ with computer simulation "measurement" of τ_{avg}, for tablets in flows with different μ and U, but with fixed orientation, size D and material property τ_u.

From the mathematical form of g, the tablet erosion model is obtained by multiplying g by $\tau_{avg}D^2/U$.

REFERENCES

1. A. Lindahl, A. L. Ungell, L. Knutson, and H. Lennernas. Characterization of fluids from the stomach and proximal jejunum in men and women. *Pharm. Res.* **14**:497–502 (1997).
2. J. B. Dressman, G. L. Amidon, C. Reppas, and V. P. Shah. Dissolution testing as a prognostic tool for oral drug absorption: immediate release dosage forms. *Pharm. Res.* **15**:11–22 (1998).
3. B. Abrahamsson, K. Roos, and J. Sjogren. Investigation of prandial effects on hydrophilic matrix tablets. *Drug Dev. Ind. Pharm.* **25**:765–771 (1999).
4. D. A. Alderman. Review of cellulose ethers in hydrophilic matrices for oral controlled-release dosage forms. *Int. J. Pharm. Technol. Prod. Manuf.* **5**:1–9 (1984).
5. B. Abrahamsson, M. Alpsten, B. Bake, U. E. Jonsson, M. Eriksson-Lepkowska, and A. Larsson. Drug absorption from nifedipine hydrophilic matrix extended-release (ER) tablet-comparison with an osmotic pump tablet and effect of food. *J. Control. Release* **52**:301–310 (1998).
6. M. Kamba, Y. Seta, A. Kusai, M. Ikeda, and K. Nishimura. A unique dosage form to evaluate the mechanical destructive force in the gastrointestinal tract. *Int. J. Pharm.* **208**:61–70 (2000).
7. L. E. Dahlinder, C. Graffner, and J. Sjogren. Strength of the insoluble residues of plastic matrix slow release tablets (Duretter) in vitro and in vivo. *Acta Pharm. Suec.* **10**:323–332 (1973).
8. M. Shameem, N. Katori, N. Aoyagi, and S. Kojima. Oral solid controlled release dosage forms: role of GI-mechanical destructive forces and colonic release in drug absorption under fasted and fed conditions in humans. *Pharm. Res.* **12**:1049–1054 (1995).
9. B. Abrahamsson, M. Alpsten, B. Bake, A. Larsson, and J. Sjogren. *In vitro* and *in vivo* erosion of two different hydrophilic gel matrix tablets. *Eur. J. Pharm. Biopharm.* **46**:69–75 (1998).
10. A. Pal, K. Indireshkumar, W. Schwizer, B. Abrahamsson, M. Fried and J. G. Brasseur, Gastric flow and mixing studied using computer simulation. *Proc. R. Soc. Lond. B Biol. Sci.* **271** (2004).
11. A. Pal, B. Abrahamsson, W. Schwizer, G. S. Hebbard, and J. G. Brasseur. Application of a virtual stomach to evaluate gastric mixing and breakdown of solid food. *Gastroenterology* **124**:A673–A674 (2003).
12. R. L. Panton. *Incompressible Flow*, John Wiley & Sons, New York, 1996.
13. K. Indireshkumar, J. G. Brasseur, H. Faas, G. S. Hebbard, P. Kunz, J. Dent, C. Feinle, M. J. Li, P. Boesiger, M. Fried, and W. Schwizer. Relative contributions of "pressure pump" and "peristaltic pump" to gastric emptying. *Am. J. Physiol. Gasterointest. Liver Physiol.* **278**:G604–G616 (2000).
14. N. Pallotta, M. Cicala, C. Frandina, and E. Corazziari. Antropyloric contractile patterns and transpyloric flow after meal ingestion in humans. *Am. J. Gastroenterol.* **93**:2513–2522 (1998).
15. J. L. Baxter, J. Kukura, and F. J. Muzzio. Hydrodynamics-induced variability in the USP apparatus II dissolution test. *Int. J. Pharm.* **292**:17–28 (2005).
16. J. Kukura, J. L. Baxter, and F. J. Muzzio. Shear distribution and variability in the USP Apparatus 2 under turbulent conditions. *Int. J. Pharm.* **279**:9–17 (2004).
17. K. Wingstrand, B. Abrahamsson, and B. Edgar. Bioavailability from felodipine extended-release tablets with different dissolution properties. *Int. J. Pharm.* **60**:151–156 (1990).
18. B. Abrahamsson, M. Alpsten, M. Hugosson, U. E. Jonsson, M. Sundgren, A. Svenheden, and J. Tolli. Absorption, gastrointestinal transit, and tablet erosion of felodipine extended-release (ER) tablets. *Pharm. Res.* **10**:709–714 (1993).
19. L. Karlson, S. Nilsson, and K. Thuresson. Rheology of an aqueous solution of an end-capped poly(ethylene glycol) polymer at high concentration. *Colloid Polym. Sci.* **277**:798–804 (1999).
20. J. D. Sartor and C. E. Abbott. Prediction and measurement of the accelerated motion of water drops in the air. *J. Appl. Meteorol.* **14**:232–239 (1975).
21. F. M. White. *Fluid Mechanics*, McGraw-Hill, Boston, 2003.